American Mineralogist, Volume 65, pages 1220–1232, 1980

Oscillatory zoning of a discontinuous solid-solution series: sphalerite–stannite

I. S. OEN, P. KAGER

Geologisch Instituut der Universiteit van Amsterdam
Nieuwe Prinsengracht 130
1018 VZ Amsterdam, The Netherlands

AND C. KIEFT

Netherlands Organization for the Advancement of Pure Research (Z.W.O.)
c/o Instituut voor Aardwetenschappen VU
Box 7161, 1007 MC Amsterdam, The Netherlands

Abstract

Color zoning in sphalerite in a mineralized vug at the J. Cesar Mine, Cartagena, Spain, correlates with oscillatory variation in Fe, Cu, Sn, and In contents. The crystals show the following zonal units: (a) core of oscillatory-zoned sphalerite with stannite blebs, (b) conspicuous stannite zone, (c) oscillatory-zoned sphalerite with intercalated stannite zones, (d) oscillatory-zoned sphalerite with Cu,In-rich zones, (e) oscillatory-zoned sphalerite with decreased Fe, Cu, Sn, and In contents, and (f) rim zone of almost pure sphalerite.

The oscillatory zoning is explained by a crystallization model depicting cyclic supersaturation at crystal–liquid interfaces due to changes in diffusion and growth-controlled concentration gradients in the boundary layer adjacent to growing crystals during isothermal nonequilibrium crystallization of a supercooled hydrothermal solution. Rapid crystallization eliminates supersaturation at the crystal–liquid interfaces and causes a pause in crystal growth, during which renewed supersaturation of the interface liquid is attained by solute diffusion from the bulk liquid, resulting in a new growth cycle. The model involves true supercooling of bulk liquid as the driving force behind the oscillations and "constitutional supercooling" of interface liquid as the mechanism by which oscillations are accomplished.

Sphalerite and stannite form limited solid solutions in the $(Zn,Fe)S–Cu_2FeSnS_4–CuInS_2$ system, and the pseudoternary diagram for hydrothermal crystallization presumably shows a transition curve at which sphalerite forms through a peritectic reaction involving stannite and residual solution. Oscillatory-zoned stannite–sphalerite in units (a), (b), and (c) is formed by isothermal oscillatory crystallization at a temperature near the stannite–sphalerite boundary temperature. Oscillatory-zoned sphalerite in units (d) and (e) is crystallized at lower temperatures. Indium enrichment in sphalerite in unit (d) is related to the intermediate stage of fractional oscillatory crystallization, whereas low Fe, Cu, Sn, and In in sphalerite in unit (e) and almost pure sphalerite in unit (f) are related to the later stages.

Introduction

The Tertiary subvolcanic–hydrothermal lead–zinc deposits at J. Cesar Mine, Cartagena, Spain, form replacements, impregnations, veins, and nests in altered carbonaceous, pelitic, and quartzitic host rocks (Oen *et al.*, 1975). Mineralized vugs show a characteristic paragenetic sequence. The vug walls show a coating of clay minerals, pyrite, and euhedral quartz. On this coating are mm-sized crystals of sphalerite, sometimes accompanied by galena. Dendritic pyrite and marcasite form overgrowths on quartz, sphalerite, and galena. Siderite occurs as the latest vug-filling mineral.

In thin section the sphalerite shows a fine euhedral zoning of brownish and yellow zones. A sample of quartzitic schist shows a vug with euhedrally-zoned sphalerite with intercalated zones of stannite. This paper is concerned with these unusual sphalerite–stannite crystals.

0003–004X/80/1112–1220$02.00

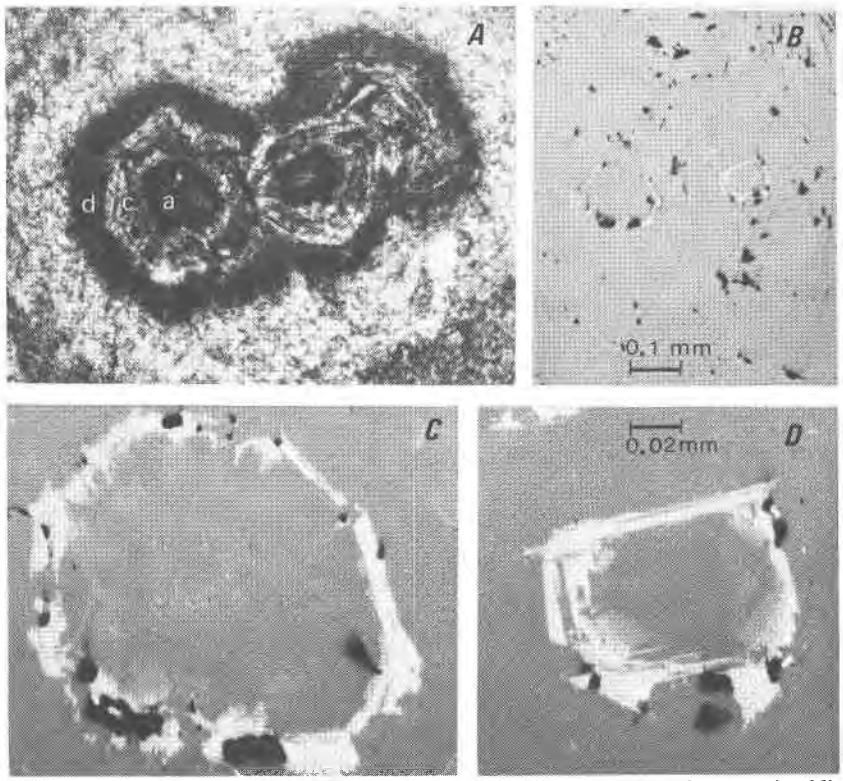

Fig. 1. Cluster of zoned sphalerite–stannite crystals. (*A*) Sphalerite zonal units (a), (c), (d), (e) in transmitted light; note coalescence of units (c), (d), and (e) of different crystals. (*B*) Stannite zonal unit (b) in reflected light. (*C*) and (*D*) Detail of zone (b); stannite forms lamellar intergrowths with sphalerite, *D* shows elimination of small crystal faces at edges of core zone by stannite.

Textural characteristics

The sphalerite–stannite crystals show a typical succession of zonal units, from the core outwards (Figs. 1–3):

(a) core of nearly opaque sphalerite with very small, often zonally arranged stannite blebs; the core zone is 0.10–0.25 mm in diameter;

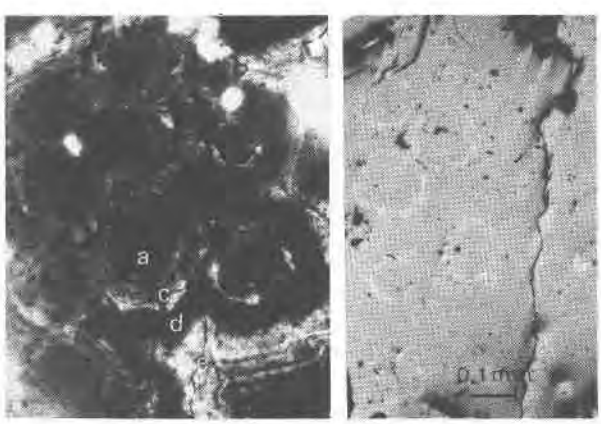

Fig. 2. Cluster of several zoned sphalerite–stannite crystals in transmitted and reflected light. Note coalescence of units (d) and (e) of different crystals.

(b) conspicuous stannite zone 0.01–0.03 mm in width;
(c) zoned brown and yellow sphalerite with intercalated thin, mostly discontinuous zones of stannite; the stannite zones decrease in thickness outwardly; width of the unit 0.1–0.3 mm;
(d) dark brown, nearly opaque sphalerite with intercalations of lighter brown sphalerite; width of the unit 0.05–0.10 mm;
(e) coarser-zoned brown and yellow sphalerite; width of the unit 0.8–1.2 mm;
(f) rim of brown sphalerite passing into an outmost zone of light yellow sphalerite; the rim zone is less than 0.05 mm wide.

Evidence that zoning and zonal units are due to successive growth zones includes: (1) oscillatory nature of the euhedral zoning as indicated by microprobe analyses (see below), (2) uniform pattern of zoning with constant width of zonal units, (3) coalescing inner zonal units overgrown by common outer zonal units (Figs. 1 and 2).

The stannite in zone (b) appears intergrown with sphalerite in a fashion suggesting that stannite began to form with oblique lamellar protrusions on small

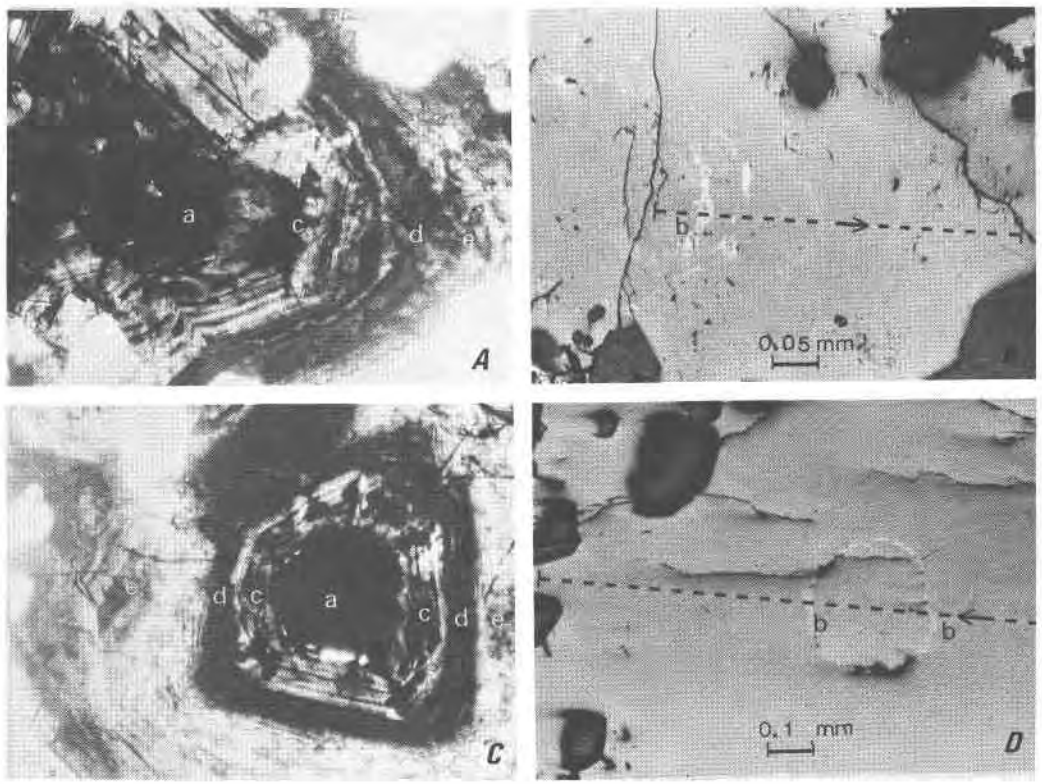

Fig. 3. Zoned sphalerite–stannite crystals. (*A*) and (*C*) Fine zoning in units (a), (c), (d), and (e) visible in transmitted light. (*B*) and (*D*) Stannite zone (b) and thin stannite zones in unit (c) in reflected light. Broken lines are traces of step traverses in Figs. 4 and 5.

faces or edges of the sphalerite crystal core, and then continued to grow in layers parallel to larger crystal faces (Figs. 1C and 1D). Sometimes the growth process has apparently resulted in elimination of small crystal faces and change of crystal morphology during growth (Fig. 1D). The intergrowth with sphalerite is interpreted as due to a peritectic reaction of stannite and solution. The stannite zone (b), and also the zonally arranged stannite blebs in core zone (a) and discontinuous thin stannite zones in unit (c), may thus be considered as growth zones in zoned sphalerite–stannite crystals. The possibility that stannite originated by later replacement processes is inconsistent with the occurrence of the mineral in a few fixed zones and with the absence of replacement veinlets and grains of stannite. The possibility that stannite was exsolved from sphalerite cannot be precluded from a textural point of view, as especially the stannite blebs in unit (a) show resemblance to exsolution blebs. However, the compositions of stannite and sphalerite are different from those that would be expected if these minerals were formed by decomposition of a solid solution (see later section).

The investigated sample shows mm-thick fractures extending from the vug across the clay minerals–pyrite–quartz coating into the vug wall. The succession of units (a) to (f) is shown by crystals on the vug wall. The small fractures contain crystals with units (c) and (d). These fracture fillings are apparently contemporaneous with the deposition of units (c) and (d) of the crystals in the vug. This time-bound deposition of zonal units is also shown by the coalescence of contemporaneous units of different crystals to one continuous zone (Figs. 1 and 2). The zonal units presumably reflect changes with time in temperature–pressure–composition relations in the mineral-forming solutions. Other samples from the same locality show sphalerite with units (d), (e), and (f), or (e) and (f). These represent the commonly occurring sphalerite, which differs from the unusual sphalerite–stannite crystals by the absence of stannite-bearing inner units. The latter units presumably reflect an early stage in the crystallization of the sphalerite.

Composition of zonal units

Microprobe step traverses across the zoning were obtained with a Cambridge Instrument Co. fully-automated Mark 9 microprobe, operated at an acceleration potential of 15 kV, using $K\alpha$ lines for Fe, Mn, Zn, Cu, S, and $L\alpha$ lines for Sn, Cd, and In. Data

were taken at steps of 3 microns for detailed traverses and of 10, 20, or 40 microns for gross traverses. In each traverse all elements were measured at the same points with counting times 3 seconds. At selected places point analyses were made with counting times to 25 seconds. Standards used were pure metals for Fe, Zn, Cu, Cd, and In, synthetic SnS for Sn, analyzed rhodonite for Mn, and analyzed pyrite for S. Raw data were corrected for matrix effects according to the Mark 9 on-line ZAF-correction computer program. Results of point analyses were used to calibrate the step traverses; for each step weight and atomic percentages were calculated.

Since the zones are often less than 1 micron in width, the true maxima and minima are located in the step traverses only by chance. Nevertheless, oscillatory zoning is revealed by 3- and 10-micron step traverses, and is discernible even in the 20- and 40-micron step traverses, by the oscillation of data around an average (Figs. 4 and 5). Another disadvantage is that points on or near zone boundaries, polishing scratches, and pits give inaccurate results. Although the step traverses are not an exact replica of the zoning, they consistently reveal a pattern of chemically characterized units corresponding to the optically distinguished units (a) to (f).

Microprobe analyses show 0.05–0.15 wt% Mn and about 0.15 wt% Cd in the sphalerite. These are neglected in the step traverses, which show that the zoning is related to variation in Fe, Cu, Sn, and In. Figures 4 and 5 are examples of step traverses across the zoned crystals. The compositions of units (a) to (f) as deduced from several traverses and point analyses are summarized in Table 1. Significant characteristics include the following points.

(1) Oscillatory variation of Fe, Cu, and Sn in sphalerite around outwardly decreasing values; Fe oscillates around average values, decreasing from 8.7 at.% in unit (a) to about 6.0 at.% in the outer part of unit (e); Cu and Sn oscillate sympathetically around average values, decreasing from 0.9 at.% Cu and 0.5 at.% Sn in unit (a) to 0.15 at.% Cu and 0.05 at.% Sn in unit (e). The outward decrease in Cu and Sn is also clearly shown by Cu and Sn microprobe X-ray images of zoned crystals (Fig. 6).

(2) The sphalerite zoning is complicated by zones of stannite in units (a), (b), (c), and of Cu,In-rich sphalerite in unit (d).

(3) In the step traverses the Cu, Sn, and In peaks marking stannite zones in units (b) and (c) generally decrease in height outwardly. This is ascribed to outwardly increasing fineness of the stannite zones and not to differences in stannite composition (Figs. 4 and 5). In a few cases it can be shown by detailed scans that stannite in units (c) and (b) has approximately similar composition, and similarity in composition of the stannite in units (a), (b), and (c) is further assumed.

(4) The broad stannite zone (b), which presumably marks a stage of accelerated stannite growth, is typically followed by a sphalerite zone showing a clear Cu–Sn minimum (Figs. 4 and 5).

(5) Indium is concentrated in stannite and in unit (d) in Cu,In-rich sphalerite containing an average of 2.3 mol% and a maximum of 4.9 mol% $CuInS_2$ (see also Fig. 6). The Cu–In and Cu–Sn maxima and minima in unit (d) do not coincide.

(6) The rim zone (f) shows a sharp drop in Fe, Cu, and Sn in sphalerite, and the outermost zone of the crystals consists of almost pure sphalerite.

(7) Cu and Sn in sphalerite are close to 2:1 in atomic proportions; the average compositions of sphalerite and stannite can be expressed as solid solutions of (Zn,Fe)S, Cu_2FeSnS_4, and $CuInS_2$ (Table 1).

(8) Sphalerite low in Fe, Cu, Sn, and In is light yellow transparent (rim zone); sphalerite high in Fe, Cu, and Sn or in Fe, Cu, and In is nearly opaque to dark brown [unit (a) and unit (d), respectively]; sphalerite low in Sn and In but containing appreciable Fe is brownish yellow [unit (e)].

A model for oscillatory crystallization

Zoning in minerals can be explained by various causes, including recurrent changes in pressure–temperature–composition conditions of mineral-forming fluids, deposition from colloidal gels, solid state reactions involving decomposition of solid solutions, diffusion and replacement reactions, and metamorphic growth. However, there is strong evidence that oscillatory zoning, for example in magmatic plagioclase (Bottinga *et al.,* 1966; Sibley *et al.,* 1976) and hydrothermal sphalerite (Roedder, 1968), is mostly due to variation in growth rate of crystals and diffusion rate of solute in the liquid ahead of growing crystals.

In this paper oscillatory crystallization of sphalerite–stannite solid solutions from hydrothermal solution is described by a crystallization model similar to the diffusion and growth-controlled model proposed by Sibley *et al.* (1976) for oscillatory zoned magmatic plagioclase. Although Sibley *et al.* use the term constitutional supercooling to imply "varying degrees of supersaturation due to concentration gradients in a melt as opposed to 'supercooling' which implies su-

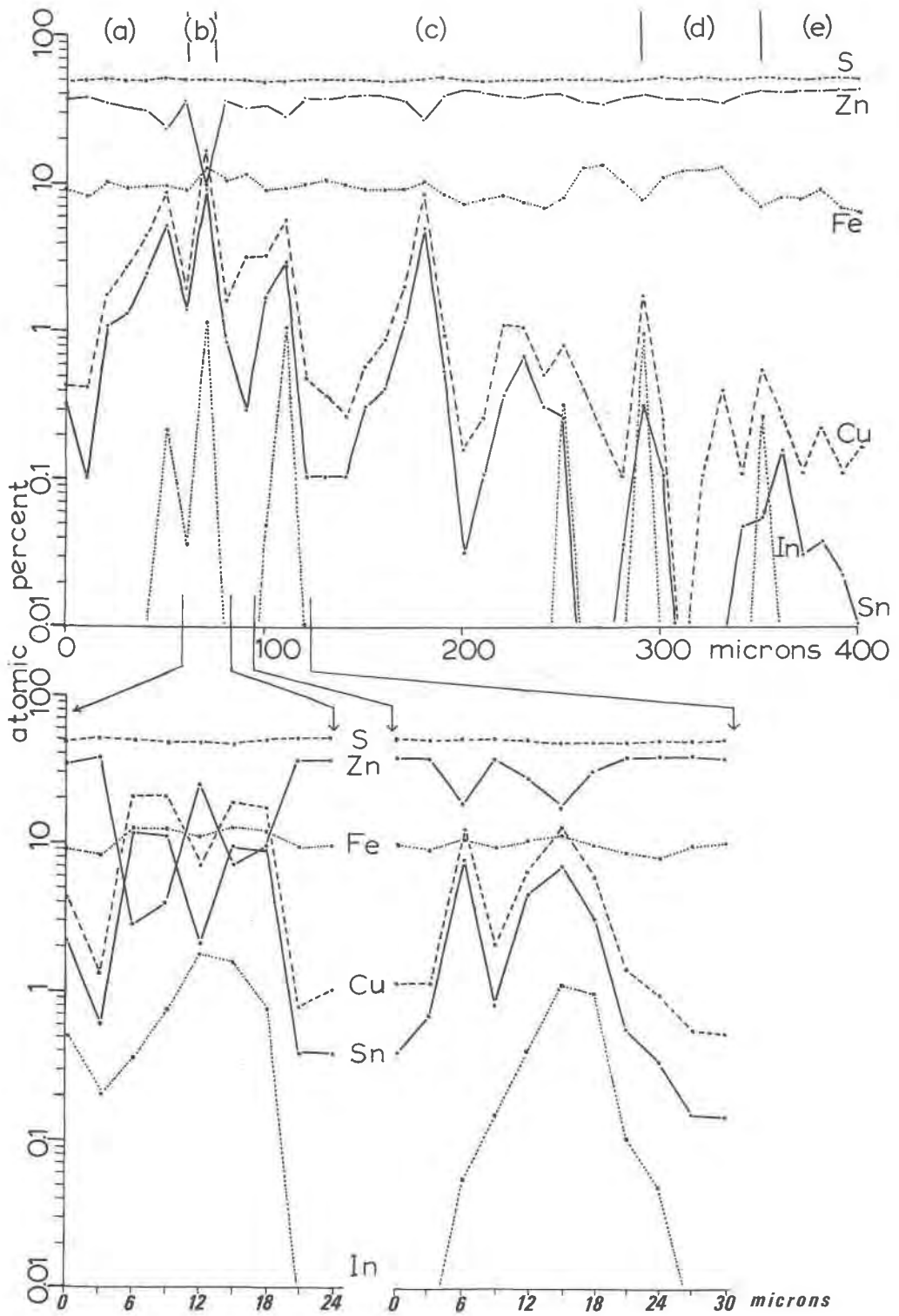

Fig. 4. Upper figure is a 10-micron microprobe step traverse across units (a) to (e) of the crystal in Fig. 3*A–B*. Stannite zones are characterized by Cu–Sn–In peaks; thin stannite zones in unit (c) show lower peaks than stannite zone (b), due to the fineness of these zones and not because of compositional differences. Lower figures are 3-micron detailed traverses across the indicated stannite zones; zone (b) shows two Cu and Sn peaks, between which the analysis is clearly contaminated by intergrown sphalerite (Fig. 3*B*). The stannite zone next to zone (b) shows higher Cu and Sn in the 3-micron than in the 10-micron traverse. Spot analyses indicate an approximately uniform stannite composition.

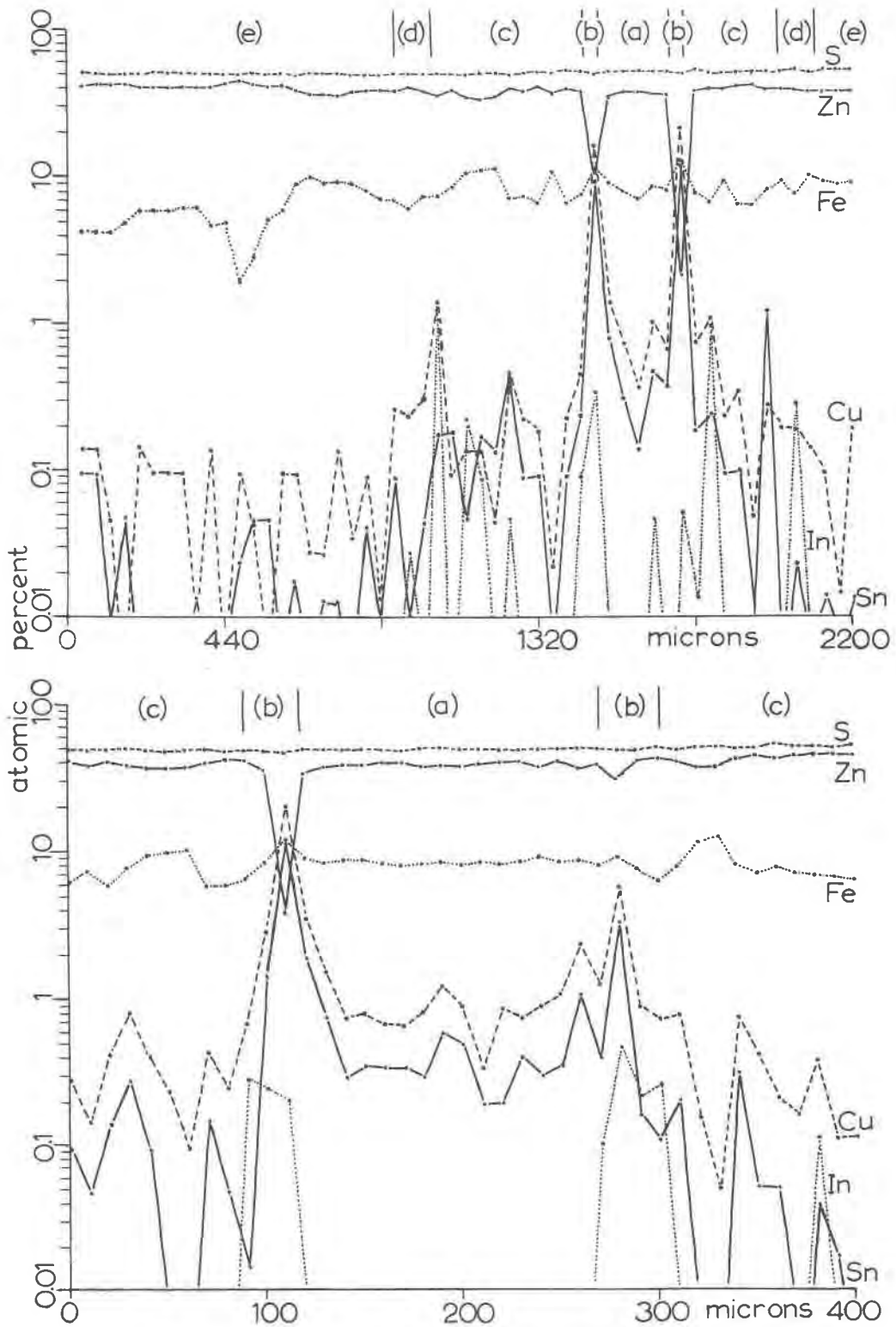

Fig. 5. Upper figure is a 40-micron step traverse; the trace of the right half of the traverse is shown in Fig. 3*D*. Lower figure is a 10-micron step traverse across another sphalerite–stannite crystal; stannite zone (b) is of uniform composition and the lower Cu and Sn peaks at the right are clearly due to contamination by sphalerite. Note Cu and Sn minima adjoining zone (b).

Table 1. Composition of zonal units

Zonal unit (a)

Oscillatory zoned nearly opaque sphalerite:

	oscillating between	average	average molecular composition	
S	49.4-53.9 at.%	50.9 at.%	ZnS	81.8 mol.%
Zn	36.0-41.0 "	39.0 "	FeS	17.2 "
Fe	7.5- 9.5 "	8.7 "	Cu_2FeSnS_4	1.0 "
Cu	0.1- 1.6 "	0.9 "		
Sn	0.1- 0.9 "	0.5 "		
In	< 0.02 "			

Some higher Cu, Sn and In peaks in step traverses are due to small stannite blebs.

Zonal unit (b)

Stannite:

		average molecular composition	
S	50.0 ± 1.0 at.%	Cu_2FeSnS_4	64.8 mol.%
Zn	4.3 ± 0.6 "	ZnS	24.4 "
Fe	12.5 ± 1.1 "	FeS	6.3 "
Cu	21.0 ± 1.0 "	$CuInS_2$	4.5 "
Sn	11.4 ± 0.2 "		
In	0.8 ± 0.4 "		

Zonal unit (c)

Oscillatory zoned brown and yellow sphalerite:

	oscillating between	average	average molecular composition	
S	49.3-52.8 at.%	50.8 at.%	ZnS	84.2 mol.%
Zn	39.0-44.0 "	41.0 "	FeS	15.3 "
Fe	6.0-10.0 "	7.5 "	Cu_2FeSnS_4	0.5 "
Cu	0.0- 0.9 "	0.5 "		
Sn	0.0- 0.7 "	0.2 "		
In	< 0.02 "			

Step traverses show a pronounced Cu-Sn-minimum corresponding to a zone of yellow sphalerite following unit (b). Stannite zones in unit (c) are of similar composition as unit (b), but are marked in step traverses by Cu, Sn and In peaks lower than those of unit (b) because of fineness of the zones.

Zonal unit (d)

Dark zones in oscillatory zoned dark and light brown sphalerite:

	oscillating between	average	average molecular composition	
S	49.5-53.0 at.%	50.5 at.%	ZnS	81.1 mol.%
Zn	34.6-41.0 "	39.0 "	FeS	16.2 "
Fe	6.5- 8.5 "	8.0 "	$CuInS_2$	2.3 "
Cu	0.2- 2.8 "	1.5 "	Cu_2FeSnS_4	0.4 "
Sn	0.0- 0.9 "	0.2 "		
In	0.3- 2.3 "	0.8 "		

Light brown zones are intermediate in composition between sphalerite of units (c) and (e). In the step traverses the Sn and In maxima do not coincide.

Zonal unit (e)

Oscillatory zoned brown and yellow sphalerite:

	oscillating between	average	average molecular composition	
S	49.0-54.0 at.%	51.0 at.%	ZnS	85.5 mol.%
Zn	37.3-44.8 "	41.3 "	FeS	14.3 "
Fe	4.5-10.0 "	7.0 "	Cu_2FeSnS_4	0.2 "
Cu	0.0- 0.9 "	0.15 "		
Sn	0.0- 0.5 "	0.05 "		
In	< 0.02 "			

Step traverses show decrease in Fe from about 8.5 at.% in the inner to about 6.0 at.% in the outer part of the unit.

Zonal unit (f)

Sharp decrease in sphalerite of Fe, Cu, Sn and In; the outer rim of yellow sphalerite contains less than 1 wt % Fe, 0.1 wt % Cu, 0.02 wt % Sn, and 0.05 wt % In.

persaturation due to temperature variations," they also state that this usage of the term differs from the original definition. The notion of constitutional supercooling as developed by metallurgists (Rutter and Chalmers, 1953; Tiller *et al.*, 1953; Tiller, 1970) refers to a case where a liquid is not supercooled, but where in a boundary layer adjacent to growing crystals supercooling is caused by the development of a compositional gradient. Because in the models of Sibley *et al.* and this paper thermal supercooling of bulk liquid is presumed, these models may strictly speaking not be referred to as constitutional supercooling models. These models in effect involve both true supercooling, which is necessary to initiate the crystallization and as the driving force behind the oscillations, and "constitutional supercooling" in the sense of Sibley *et al.*, which is the mechanism by which oscillations are accomplished.

Equilibrium crystallization involves the condition that at the temperature of crystallization liquid and solid phases have the homogeneous compositions indicated by liquidus and solidus in the equilibrium diagram. Homogeneity of composition must be maintained by diffusion processes that are relatively slow, and therefore crystallization often proceeds under nonequilibrium conditions with concentration and possibly also temperature gradients in a boundary layer adjacent to growing crystals. For the zoned

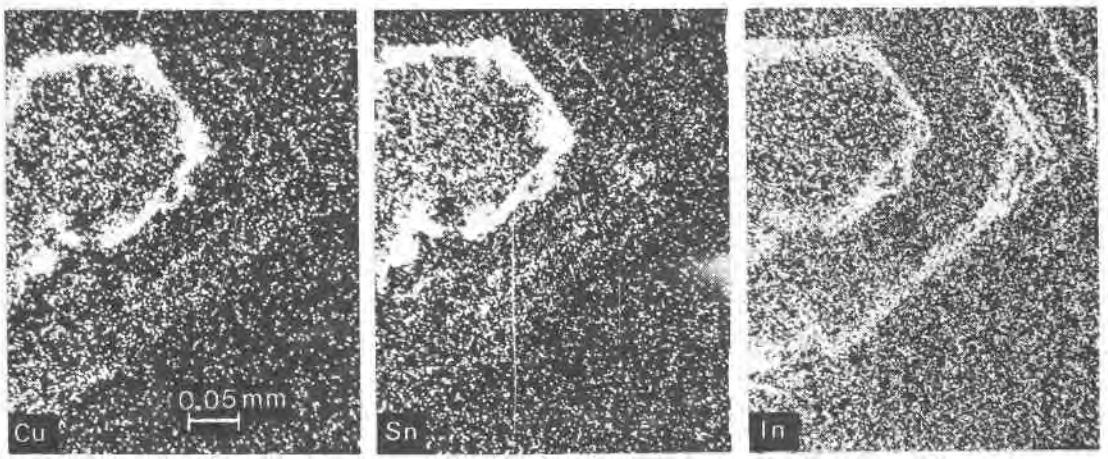

Fig. 6. Cu$K\alpha$, Sn$L\alpha$, and In$L\alpha$ microprobe X-ray images of a zoned sphalerite–stannite crystal. Stannite zone (b) is characterized by Cu, Sn, and In concentrations; sphalerite of unit (d) shows concentration of In. Note decreasing Cu and Sn in units (a), (c), and (e).

sphalerite–stannite crystals nonequilibrium crystallization from a hydrothermal solution that has entered cavities in cooler wall rock is considered. In view of the many parameters to be considered in a quantitative treatment and of which detailed knowledge is not available (see *e.g.,* Toulmin and Clark, 1967), a qualitative approach that necessarily involves some extent of simplification and conjecture is followed below.

Oscillatory crystallization of a binary solid solution AB from a supercooled liquid in a cavity is considered in Figure 7. The composition of the solid crystallizing from supercooled liquid cannot be predicted exactly, as it will be controlled by a metastable solidus and will differ from the equilibrium composition at the temperature of crystallization. Thus, in Figure 7 the initial solid that will nucleate on the cavity wall from supercooled liquid d at temperature T_7 may have composition B_7', located on a metastable solidus and connected by a metastable isothermal tie line with liquid d; B_7' will fall somewhat to the left of the equilibrium composition B_7 at T_7. The crystal nuclei will become bounded by a liquid layer, which through extraction of B_7' is shifted in composition from d towards L_7 on the liquidus. As the boundary liquid moves away from d, the precipitating solid changes from B_7' towards B_7, while due to crystallization the bulk liquid is displaced towards d'. Figure 7a depicts the initial situation with at T_7 solid B_7' bounded by a liquid layer showing a gradient of compositions between those of the interface liquid moving towards L_7 and the bulk liquid moving towards d'. If during nucleation the temperature decreases continuously to T_9, the interface liquid will move towards the liquidus, following for example path d–L_8–L_9, while precipitating crystal zones B_7'–B_8–B_9. If then the temperature along the cavity wall remains stationary at T_9, crystallization will cease by the time the interface liquid reaches L_9 and equilibrium is established at the crystal–liquid interface between solid B_9 and liquid L_9 (see also Fig. 7b). During the cessation of crystal growth, solute diffusion tends to eliminate the concentration gradient in the boundary layer and causes the interface liquid L_9 to be moved back, off the liquidus, in the direction of the supercooled bulk liquid d' (see also Fig. 7c). While migrating off the liquidus at constant temperature the interface liquid becomes increasingly supercooled ("constitutionally supercooled" in the sense of Sibley *et al.,* 1976) with respect to its liquidus temperature. If we assume that the crystals grow in faceted steps with smooth interfaces (and not with diffuse interfaces, see Chalmers, 1964, and Sibley *et al.,* 1976) the interface liquid may migrate a certain distance L_9–L_9' off the liquidus before at L_9' supercooling of the interface liquid becomes sufficient to initiate a new growth cycle. Again the composition of the solid that crystallizes at T_9 from supercooled interface liquid L_9' will fall near B_9' on a metastable solidus somewhat to the left of equilibrium composition B_9. As crystallization of B_9' sets in, the interface liquid is depleted in B_9' and moves back again to L_9, while depositing crystals B_9'–B_9. Complications may arise if supply of latent heat of crystallization of $B_9'B_9$ exceeds the rate of heat dissipation, resulting in local and temporary temperature increase around centers of crystallization. In the latter case the interface liquid and crystallizing solid may describe paths that loop upward in temperature, for example L_9'–L_8–L_9 and B_9'–B_8–B_9, respectively. Figure

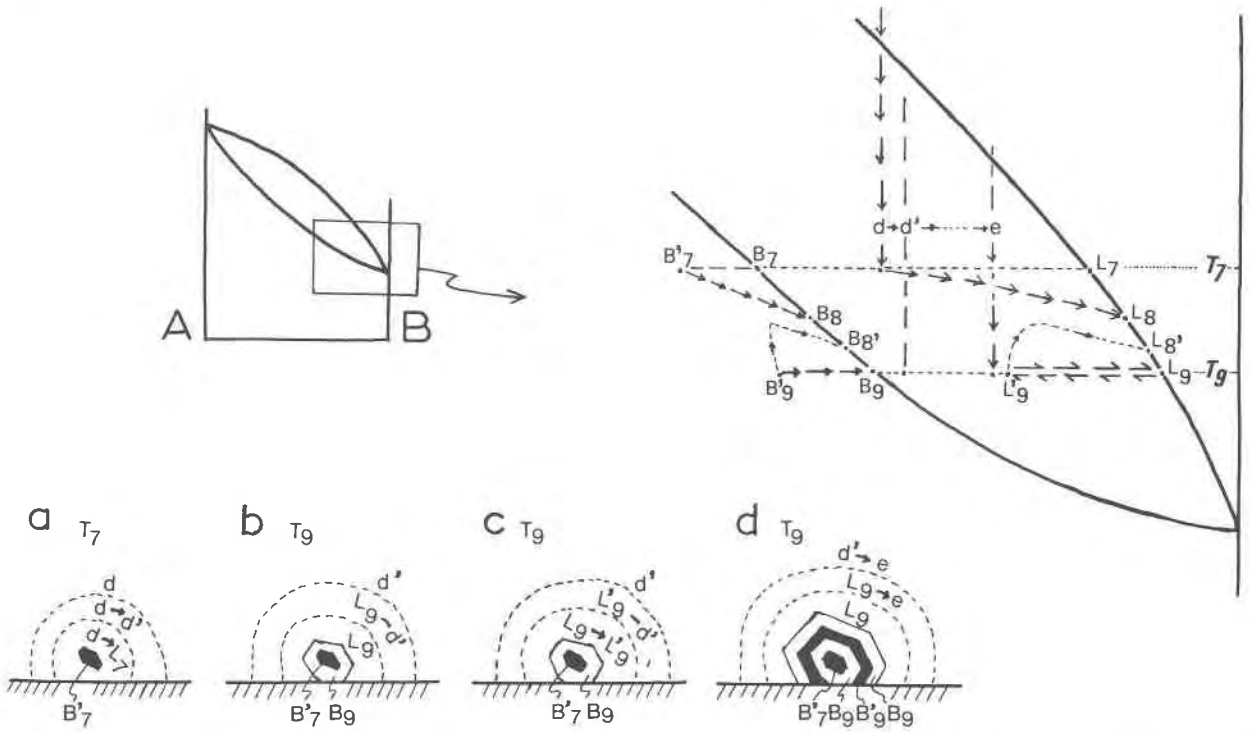

Fig. 7. Formation of oscillatory-zoned crystals of a binary continuous solid solution series AB. Isothermal oscillatory crystallization of crystal zones B'_9–B_9–B'_9–B_9 at temperature T_9 involves crystallization from an interface liquid changing cyclically along L'_9–L_9–L'_9–L_9. See text for further explanation.

7d shows the situation at the end of the growth cycle when the interface liquid is back at L_9 and in equilibrium with solid B_9 at T_9; this stage represents a new growth pause, *i.e.* the recurrence of the conditions that will lead to a new growth cycle.

As shown in Figure 7, oscillatory zoning B'_9–B_9–B'_9–B_9 results from isothermal crystallization with supercooling as the driving force. Crystallization of nuclei B'_7–B_9 occurs between T_7 and T_9 during initial supercooling of liquid d. During crystallization with crystal growth rate exceeding solute diffusion rate a liquid boundary layer with steepening gradient of decreasing supersaturation (supercooling) towards the crystal–liquid interface is developed. The interface liquid moves towards the liquidus and crystallization is arrested as at the crystal–liquid interface equilibrium is reached at T_9 between solid B_9 and liquid L_9. During the growth pause solute diffusion predominates and the interface liquid composition is moved back, off the liquidus, towards that of the supersaturated (supercooled) bulk liquid. Crystallization resumes as at L'_9 the supersaturation of the interface liquid initiates a new growth cycle B'_9–B_9. Whether heat effects of crystallization are significant or not, oscillatory crystallization B'_9–B_9–B'_9–B_9 is related to cyclic changes L'_9–L_9–L'_9–L_9 of the interface liquid, operating under constant external conditions with supercooling of the bulk liquid as the driving force. Under isothermal conditions each growth cycle shifts the bulk liquid towards a less supercooled composition and as at e the bulk liquid approaches L'_9, the diminishing supercooling will eventually prevent further oscillatory crystallization at T_9. Oscillatory crystallization may resume when supercooling of bulk liquid is re-enhanced by decrease in temperature of the system (Fig. 9).

Formation of sphalerite–stannite zoned crystals

According to our model oscillatory zoning will vary with type and shape of the equilibrium diagram. For example, the sequence of A-richer to B-richer zones in Figure 7 will be reversed if the slopes of the liquidus and solidus are reversed. The observed sphalerite–stannite zoning may be explained by conjecturing a diagram of the type as shown in Figure 8 and assuming that in this pseudobinary diagram stannite can be represented by A, iron-bearing sphalerite by B, and hydrothermal solution by L. This postulate is consistent with available data indicating a miscibility gap between sphalerite and β-stannite, broadening with decreasing temperature. At 400°C β-stannite can contain about 9 wt% or 30 mol% ZnS,

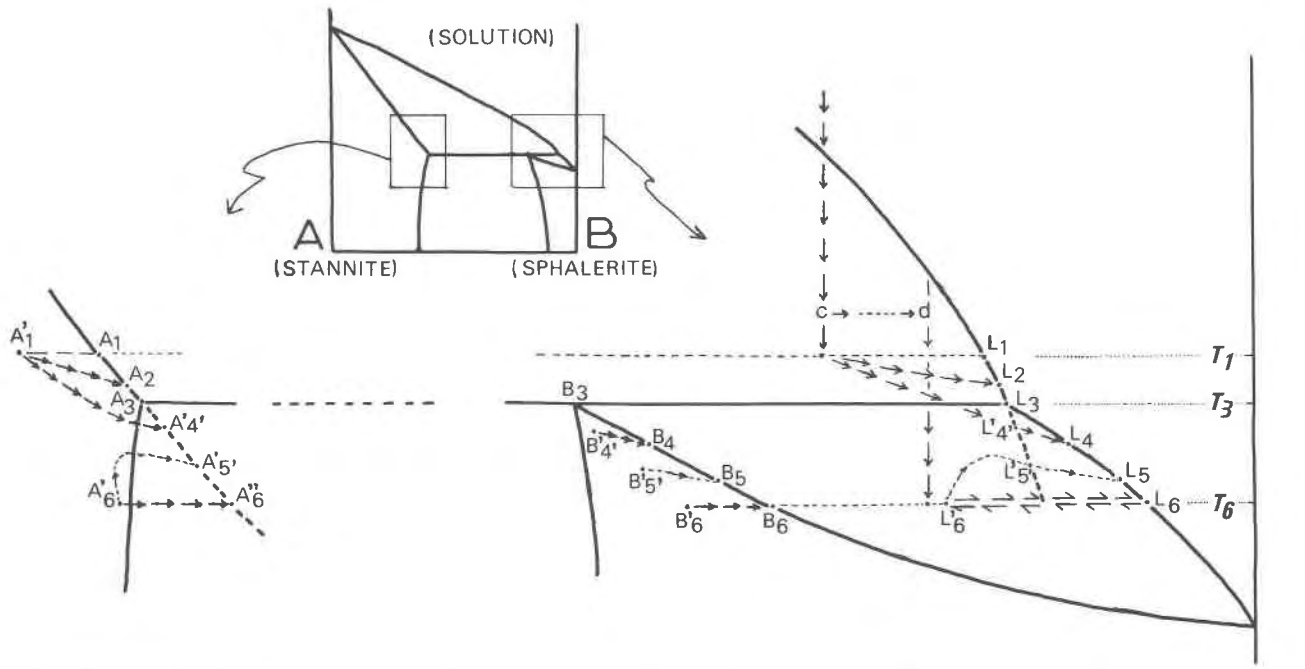

Fig. 8. Formation of oscillatory zoned crystals of a binary discontinuous solid solution series AB showing a peritectic relationship; A may represent stannite, B sphalerite. Isothermal oscillatory crystallization of crystal zones A'_6–A''_6–B'_6–B_6–A'_6–A''_6–B'_6–B_6 at temperature T_6 involves crystallization from an interface liquid changing cyclically along L'_6–L_6–L'_6–L_6. See text for further explanation.

while sphalerite can contain about 1.5 wt% or 6 mol% Cu_2FeSnS_4 (Lee, 1972; Moh, 1975). The stannite described here shows about 30 mol% (Zn,Fe)S, but the sphalerite in unit (a) contains only about 1 mol% Cu_2FeSnS_4, or less than what should be expected if the sphalerite and stannite were formed at the same temperature. According to Oen *et al.* (1975) formation temperatures of the Cartagena deposits range from above 320° to below 150°C.

In Figure 8 the nuclei crystallizing at T_1 from supercooled solution c will be of stannite A'_1, located on a metastable solidus to the left of A_1. If during nucleation the temperature decreases to T_6, the interface liquid will migrate towards L_6, following for example path c–L_2–L_3–L_6. The solid deposited from c–L_2–L_3 will be of stannite A'_1–A_2–A_3. A peritectic reaction involving stannite A_3 and interface liquid L_3 is then to occur at T_3, but with nonequilibrium crystallization this reaction may be largely overstepped and, while the interface liquid continues to move along L_3–L_6, the stannite will be overgrown by sphalerite B_3–B_6. Alternatively, the path taken by the interface liquid may be c–L'_4–L_4–L_6. The solid deposited from c–L'_4 will be of stannite A'_4–A'_4. The peritectic at the intersection with the metastable extension of the stannite phase boundary will presumably be overstepped, resulting in sphalerite B'_4–B_4–B_6 overgrowing the stannite, while the interface liquid moves further along L'_4–L_4–L_6. Whatever the path followed by the interface liquid, a growth pause will result, as at T_6 liquid L_6 and solid B_6 are in equilibrium at the crystal–liquid interface. Then the effects of solute diffusion will cause the interface liquid to be moved back off the liquidus along L_6–L'_6 until the supersaturation at L'_6 initiates a new growth cycle. The solid that crystallizes from supercooled interface liquid L'_6 must be located on the metastable leftward extension of the isothermal stable tie line L_6–B_6. As L'_6 is supersaturated with respect to stannite, deposition may begin with a stannite A'_6. As the growth cycle proceeds, the interface liquid moves again from L'_6 to L_6, while depositing stannite A'_6–A''_6 and sphalerite B'_6–B_6; the change from stannite to sphalerite crystallization occurs when the solid composition reaches the metastable peritectic on the metastable extension of the phase boundary delimiting the stannite phase field in the diagram. If crystallization is attended by significant heat effects the interface liquid and crystallizing solid may describe paths looping upward in temperature, as for example L'_6–L'_5–L_5–L_6 and A'_6–A'_5–B'_5–B_5–B_6, respectively. When the interface liquid is back at L_6 a new growth pause results and the interface liquid will start migrating back again in the reverse direction to L'_6. Oscillatory crystallization of stannite–sphalerite

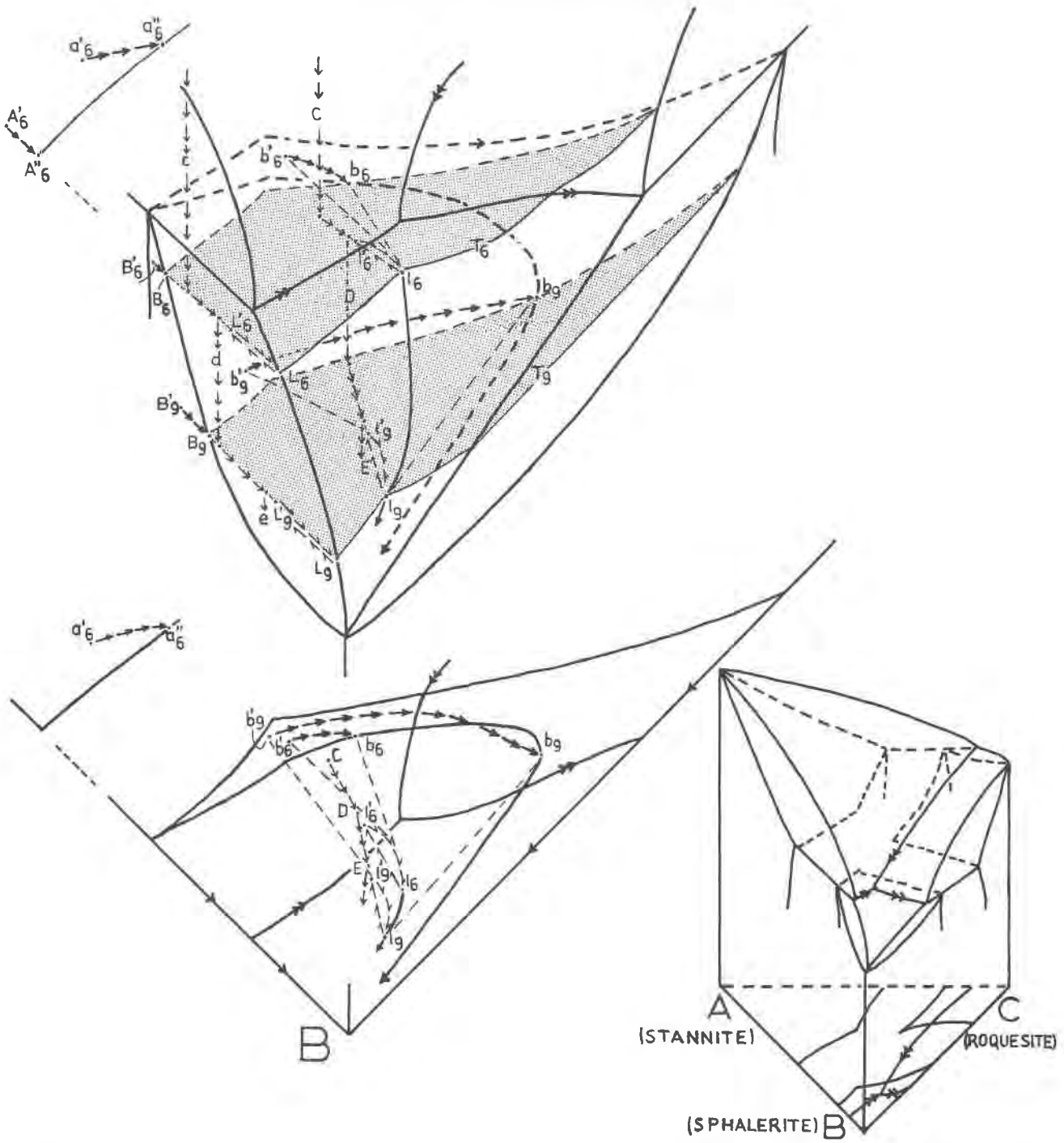

Fig. 9. Perspective sketch of equilibrium diagram, showing course of oscillatory crystallization and fractional crystallization in a ternary system with limited solid solution and peritectic relationships between components; *A* may represent stannite, *B* sphalerite, and *C* roquesite. See text for further explanation.

may continue at T_6 until the bulk liquid, which due to crystallization will be displaced from *c* towards *d*, approaches composition L'_6.

Some stannite blebs in unit (a) may represent the early stannite nuclei. Zonally arranged stannite blebs in unit (a), stannite zone (b), and discontinuous stannite zones in unit (c) represent the stannite of later growth cycles. According to the model the stannite and sphalerite compositions are determined by the solidus and metastable solidus curves and not by the

stannite–sphalerite solvus. The observation that sphalerite contains much less stannite in solid solution than might be expected if it were formed along the solvus in equilibrium with stannite is consistent with the model. The rudimentary character of most stannite zones and the intergrowth with sphalerite are presumably due to the peritectic reaction described above. An exception is the broad stannite zone (b), which is followed by a sphalerite zone with lower stannite contents than normal (see Figs. 4 and 5). This feature may represent a fluctuation in temperature. If the temperature during one growth cycle drops below T_6 in Figure 8, stannite crystallization may be extended, as the metastable extension of the stannite phase boundary is intersected at a lower temperature, while the sphalerite crystallizing at this lower temperature will also contain less stannite in solid solution.

Units (a), (b), and (c) may have crystallized isothermally at T_6. However, the absence of stannite in the outer units, the outward decrease in Fe, Cu, and Sn in sphalerite, and the concentration of In in unit (d) suggest falling temperatures during crystallization of the outer units.

If we assume that crystallization temperatures of Cu,In-rich sphalerite are intermediate between those of stannite-rich and pure sphalerite, Figure 9 may depict crystallization in the pseudoternary system stannite (A)–sphalerite (B)–$CuInS_2$ or roquesite (C)–hydrothermal solution. Figure 9 shows isothermal planes at T_6 and T_9 through the sphalerite-rich portion of the three-dimensional diagram; the intersections with side AB are the T_6 and T_9 isothermal lines in the binary diagrams of Figures 8 and 7, respectively. Crystallization of units (a), (b), and (c) involves the recurrence at T_6 of stannite–sphalerite growth cycles alternating with growth pauses. During the growth cycles the interface liquid migrates in the T_6 isothermal plane along a curved fractionation path l'_6–l_6, while precipitating stannite a'_6–a''_6 and sphalerite b'_6–b_6. These stannite and sphalerite compositions lie on curves in the stannite and sphalerite phase fields in the T_6 isothermal plane and are connected by metastable isothermal tie lines with the interface liquids along the l'_6–l_6 curve. The change from stannite to sphalerite precipitation occurs at some point along the l'_6–l_6 curve when the interface liquid becomes sufficiently rich in ZnS to precipitate sphalerite. In effect this will occur at a metastable peritectic involving phases a''_6, b'_6, and a liquid between l'_6 and l_6. When the interface liquid and solid have reached the equilibrium compositions l_6 and b_6, respectively, crystallization ceases. Diffusional changes will then shift the interface liquid back from l_6 to l'_6, resulting in a new growth cycle when l'_6 is reached. Crystallization during the growth cycles causes the bulk liquid to change from C to D; at D the diminished supercooling of the bulk liquid will eventually prevent further oscillatory growth at T_6. Oscillatory crystallization may resume with formation of unit (d) as the temperature of the system is decreased to T_9. During the growth cycles the interface liquid then migrates in the T_9 isothermal plane along a curved path l'_9–l_9, while precipitating sphalerite b'_9–b_9; b'_9 is connected with l'_9 by a metastable isothermal tie line. The compositions near b_9 correspond to that of Cu,In-rich sphalerite. As sketched in Figure 9 the Sn and In maxima in oscillatory zoned sphalerite b'_9–b_9 will not coincide and this is in agreement with the observations in unit (d).

The course of oscillatory and fractional crystallization is best shown by the basal plane projection in Figure 9. During oscillatory crystallization of stannite–sphalerite a'_6–a''_6–b'_6–b_6 in units (a) to (c), the interface liquid moves cyclically along a looping path l'_6–l_6–l'_6 in the T_6-plane, while the bulk liquid changes from C to D. Decrease in temperature to T_9 results in oscillatory crystallization of sphalerite b'_9–b_9 in In-rich unit (d) from an interface liquid that loops cyclically along l'_9–l_9–l'_9 in the T_9 plane, while the bulk liquid is further changed from D to E. The bulk liquid and interface liquid compositions change along C–D–E and l_6–l_9, respectively, towards the sphalerite corner of the diagram, and it can be inferred that further stepwise cooling may result in the formation below T_9 of unit (e) with oscillatory zoned Cu,Sn,In-poor sphalerite, and of unit (f) with almost pure sphalerite.

We conclude that units (a,b,c), (d), (e), and (f) represent successive steps of fractional crystallization of ZnS-rich, Fe,Cu,Sn,In-bearing hydrothermal solution. Each step is initiated by a decrease in temperature and involves the isothermal oscillatory crystallization of supercooled solution controlled by cyclic growth and diffusion processes at the crystal–liquid interface. The earlier stages of crystallization have resulted in In enrichment in intermediate unit (d), the later stages in decreased trace-element contents in sphalerite of the outer units.

Acknowledgments

Microprobe analyses were performed in the Instituut voor Aardwetenschappen, Vrije Universiteit, with financial and personnel support from the Netherlands Organization for the Advance-

ment of Pure Research (Z.W.O.) granted to the Working Group for Analytical Geochemistry (WACOM). The authors are grateful to directors of Peñarroya-España, S.A. for permission to study the Cartagena deposits. Special thanks are due to J.C. Fernández, geologist at Cantera Emilia, for expert guidance. Critical reviews of the manuscript by Peter J. Modreski and George W. Fisher have led to important modification of the paper and are highly appreciated.

References

Bottinga, Y., A. Kudo and D. Weill (1966) Some observations on oscillatory zoning and crystallization of magmatic plagioclase. *Am. Mineral., 51,* 792–806.

Chalmers, B. (1964) *Principles of Solidification.* Wiley, New York.

Lee, J.Y. (1972) Experimental investigation on stannite–sphalerite solid solution series. *Neues Jahrb. Mineral. Monatsh.,* 556–559.

Moh, G.H. (1975) Tin-containing mineral systems, part II: phase relations and mineral assemblages in the Cu–Fe–Zn–Sn–S system. *Chemie der Erde,* 34, 1–61.

Oen, I.S., J.C. Fernández and J.I. Manteca (1975) The lead–zinc and associated ores of La Union, Sierra de Cartagena, Spain. *Econ. Geol., 70,* 1259–1278.

Roedder, E. (1968) The noncolloidal origin of "colloform" textures in sphalerite ores. *Econ. Geol., 63,* 451–471.

Rutter, J.W. and B. Chalmers (1953) A prismatic substructure formed during the solidification of metal. *Can. J. Physics, 31,* 15–39.

Sibley, D.F., T.A. Vogel, B.M. Walker and G. Byerly (1976) The origin of oscillatory zoning in plagioclase: a diffusion and growth controlled model. *Am. J. Sci., 276,* 275–284.

Tiller, W.A. (1970) Solidification. In R.W. Cahn, Ed., *Physical Metallurgy,* revised edition, p. 403–469. North-Holland Publ. Co., Amsterdam and London.

———, K.A. Jackson, J.W. Rutter and B. Chalmers (1953) The redistribution of solute atoms during solidification of metals. *Acta Metallurgica, 1,* 428–437.

Toulmin, P., III and S.P. Clark, Jr. (1967) Thermal aspects of ore formation. In H.L. Barnes, Ed., *Geochemistry of Hydrothermal Ore Deposits,* p. 437–464. Holt, Rinehart and Winston, New York.

Manuscript received, September 4, 1979;
accepted for publication, June 2, 1980.